

Metaheuristics Set

coordinated by
Nicolas Monmarché and Patrick Siarry

Volume 10

Metaheuristics for Intelligent Electrical Networks

Frédéric Héliodore
Amir Nakib
Boussaad Ismail
Salma Ouchraa
Laurent Schmitt

Color section

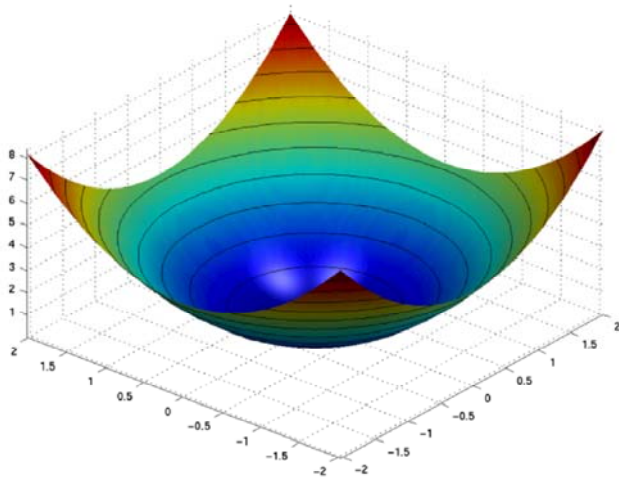


Figure 3.1. *Representation of the sphere function*

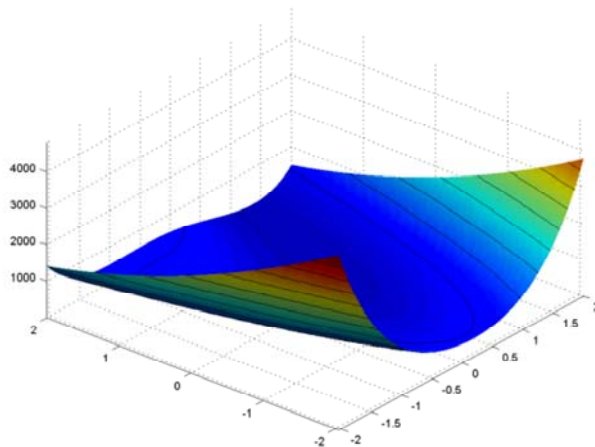


Figure 3.2. *Representation of the Rosenbrock function*

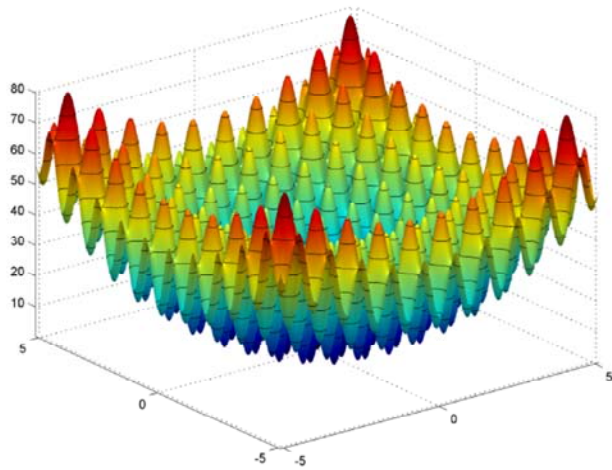


Figure 3.3. *Representation of the Rastrigin function*

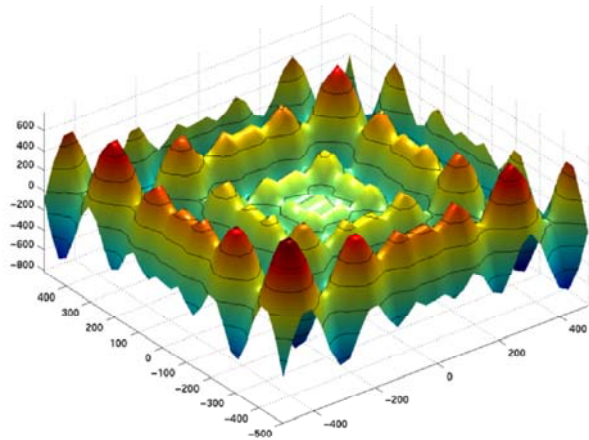


Figure 3.4. *Representation of the Schwefel function*

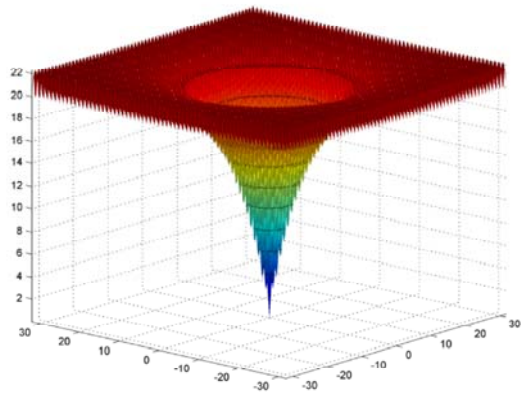


Figure 3.5. *Representation of the Ackley function*

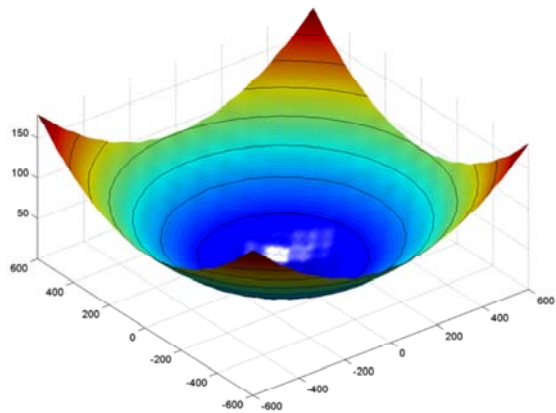


Figure 3.6. *Representation of the large-scale Griewank function*

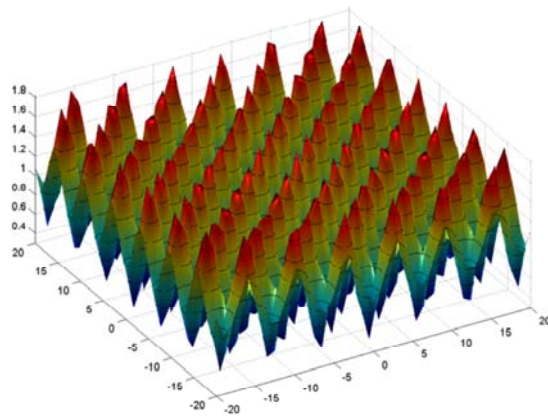


Figure 3.7. Representation of the small-scale Griewank function

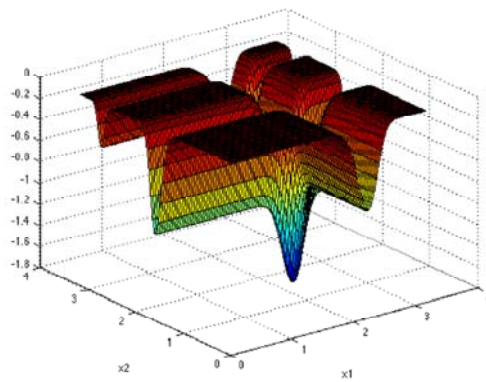


Figure 3.8. Representation of the Michalewicz function

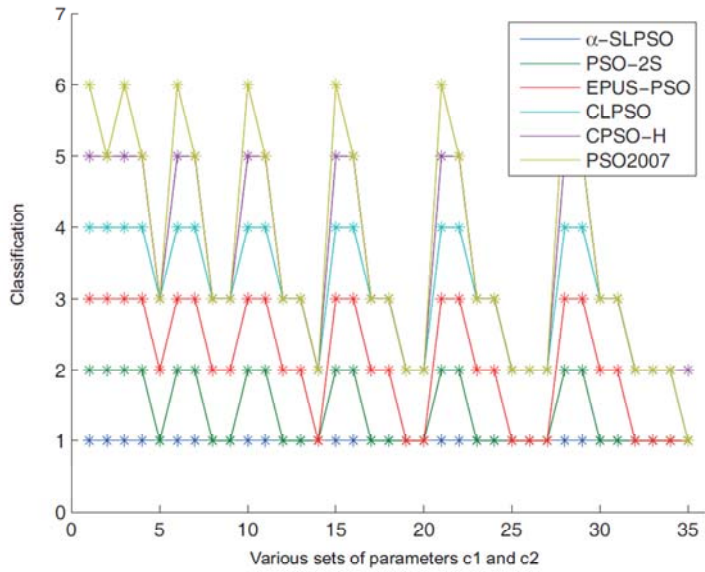


Figure 4.4. Classification of variants α -SLPSO, PSO-2S, EPUS-PSO, CLPSO, CPSO-H and the PSO2007 standard for a set of concordance parameters c_1 and c_2

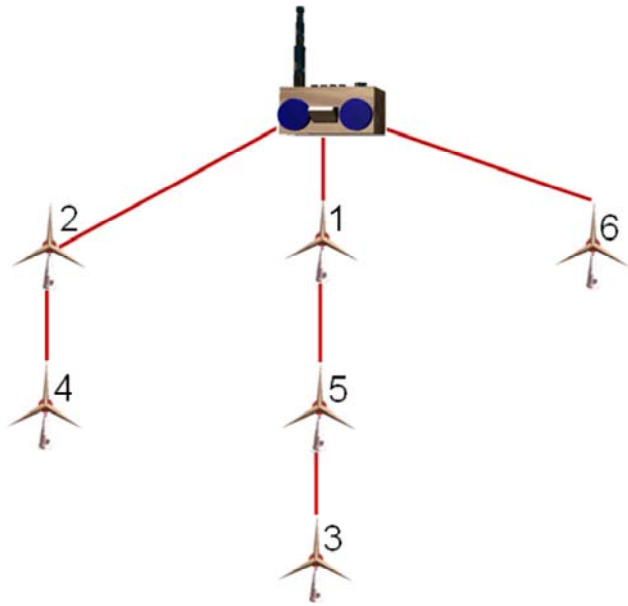


Figure 5.3. *Graph corresponding to the individual Example_Coding*

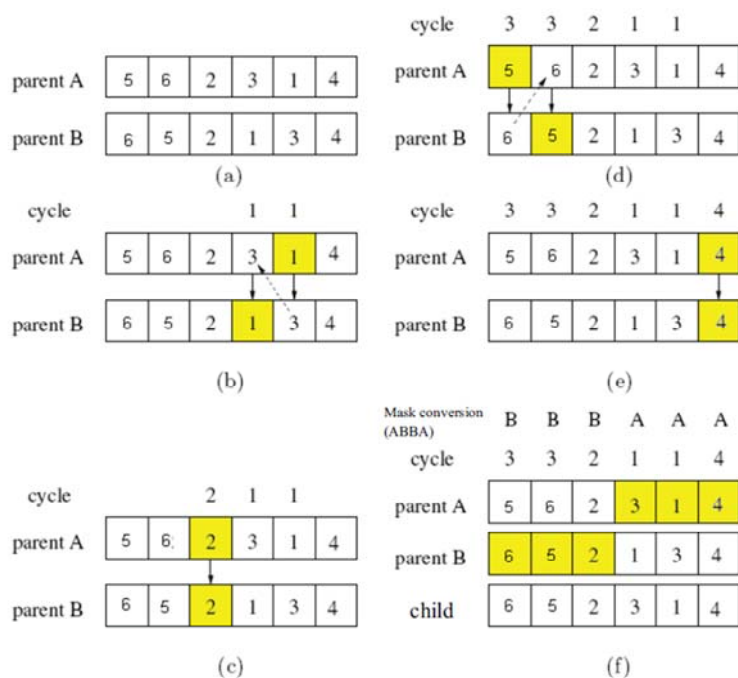


Figure 5.5. Principle of geometric crossover applied to the two parents A and B

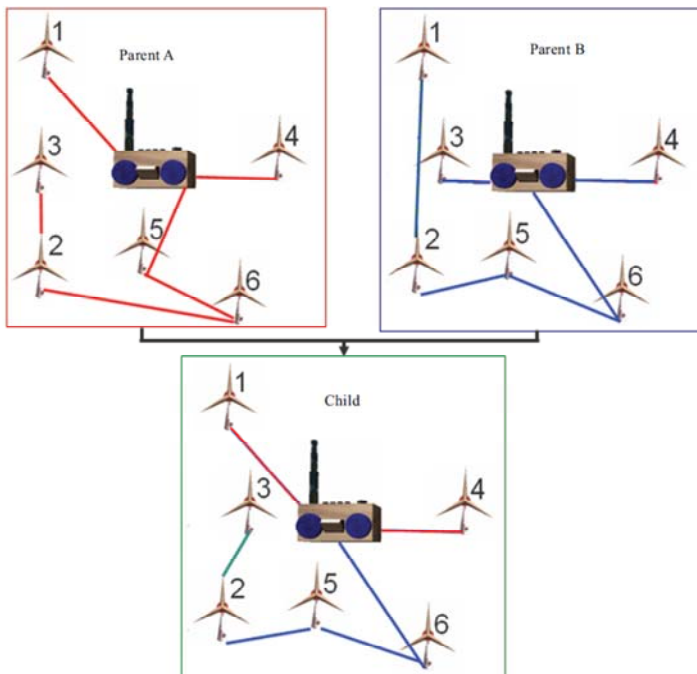


Figure 5.6. Graphical representation of the example of the crossover in Figure 5.5: a) parent A, b) parent B, and c) the child obtained by crossing over parent A and B

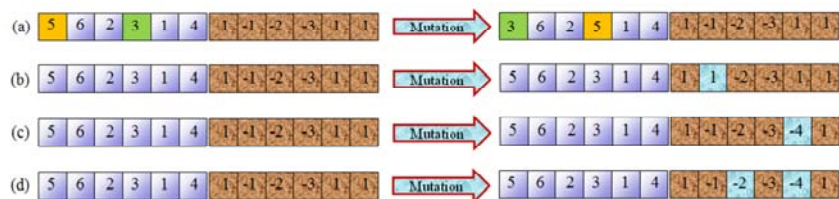


Figure 5.7. Mutation examples of an individual

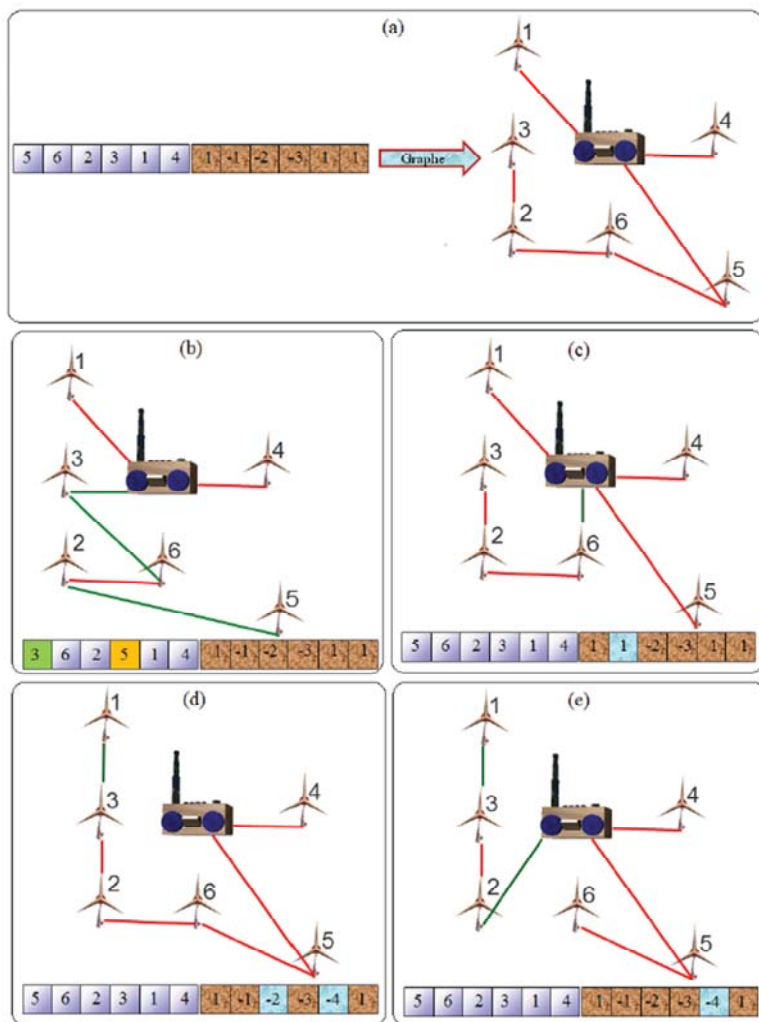


Figure 5.8. Mutation examples: a) the graph in Figure 5.7, b) modification of the turbines order in a cluster, c) addition of a cluster, d) removal of a cluster and e) modification of the number of turbines in a cluster

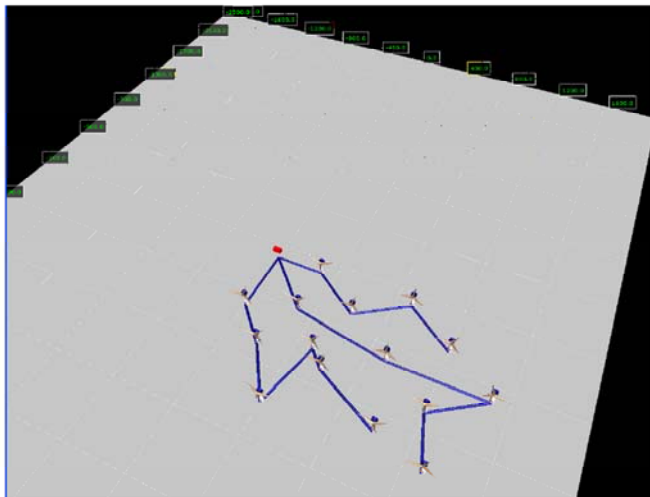


Figure 5.9. *Topology of a farm with 15 turbines obtained by the genetic algorithm*

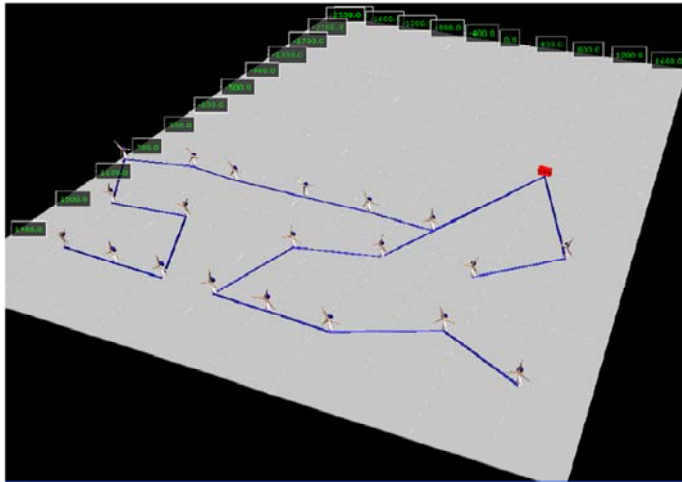


Figure 5.10. *Topology of a farm with 20 turbines obtained by the genetic algorithm*

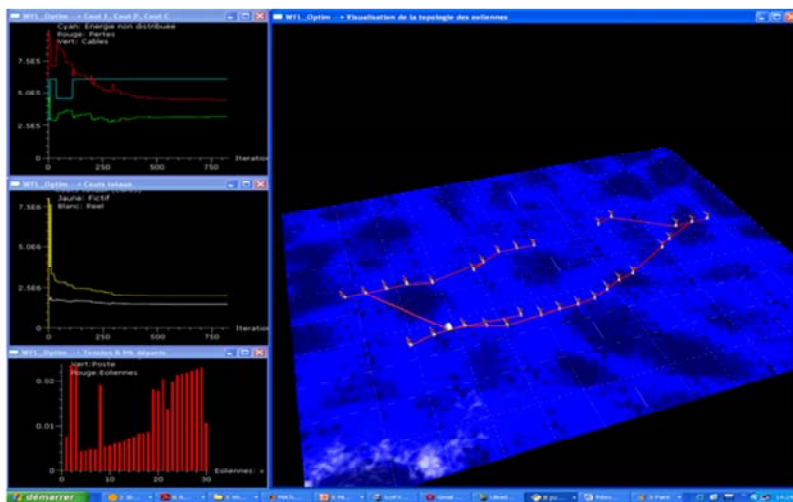


Figure 5.11. *Topology of a farm with 30 turbines obtained by the genetic algorithm*

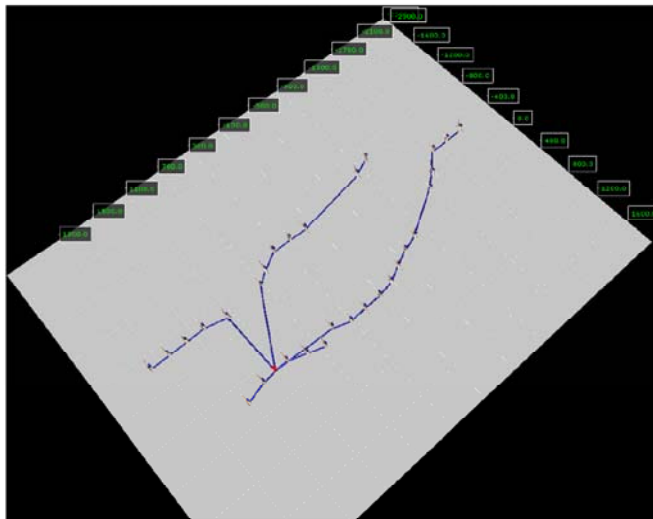


Figure 5.12. *Topology of a farm of 30 turbines proposed by human expertise*

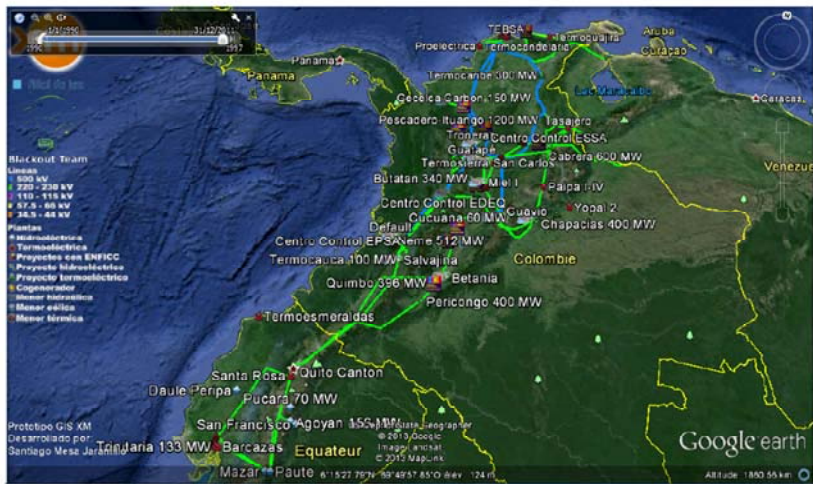


Figure 6.3. Colombian network (500 kV and 220 kV lines)
in KML file format (Google Earth)

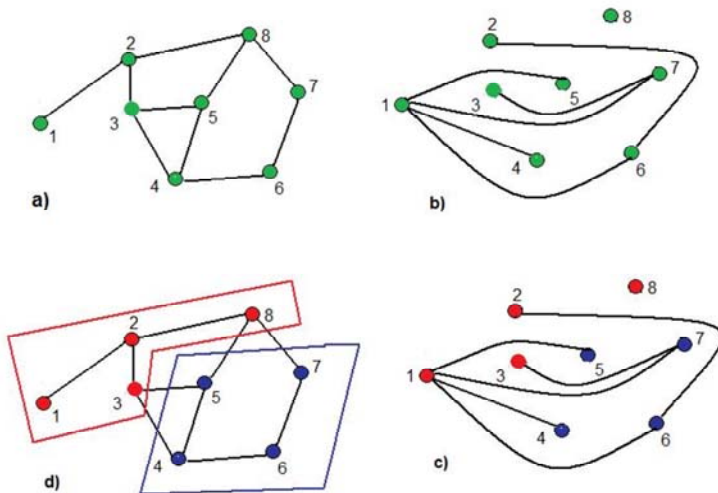


Figure 6.6. Example of the application of the coloring algorithm, $l_B = 3$: a) the initial graph G ; b) the dual graph G' ; c) solution of the coloring problem of the dual graph G' ; d) the final result (number of boxes $N_B = 2$)

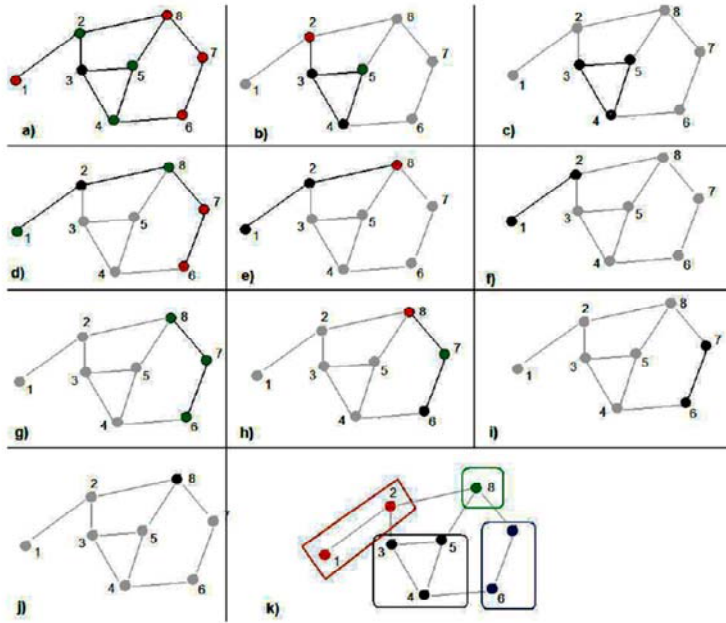


Figure 6.7. Application example of the CBB algorithm, $l_B = 2$: nodes in red correspond to nodes “set aside” (geodesic distance $\geq l_B$), in black to “central” nodes, in green to nodes that are at geodesic $< l_B$. a) Random selection of node 3 and removal of nodes at a distance $\geq l_B$ from node 3. b) Random selection of node 4 and removal of nodes at distance $\geq l_B$ from node 2. c) Selection of the remaining node 5. Iteration 1: (a)–(c). Iteration 2: d)–f). Iteration 3: g)–i). Iteration 4: j). (d) The final result (number of boxes $N_B = 4$)

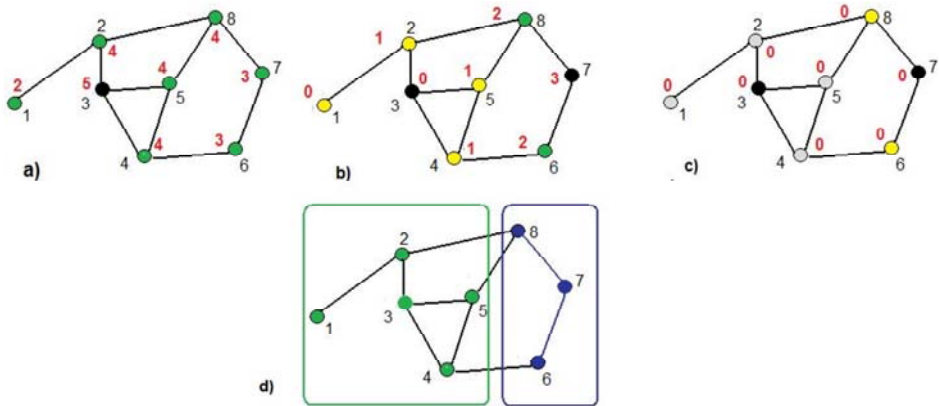


Figure 6.8. Application example of the MEMB algorithm, $r_B = 1$: nodes in green correspond to "unmarked" nodes, in yellow to "marked nodes" and black nodes to "central nodes". The gray nodes are nodes that already belong to a box. (a)–(c) Intermediate results of the MEMB algorithm; (d) final result (number of boxes $N_B = 2 =$ number of hubs)

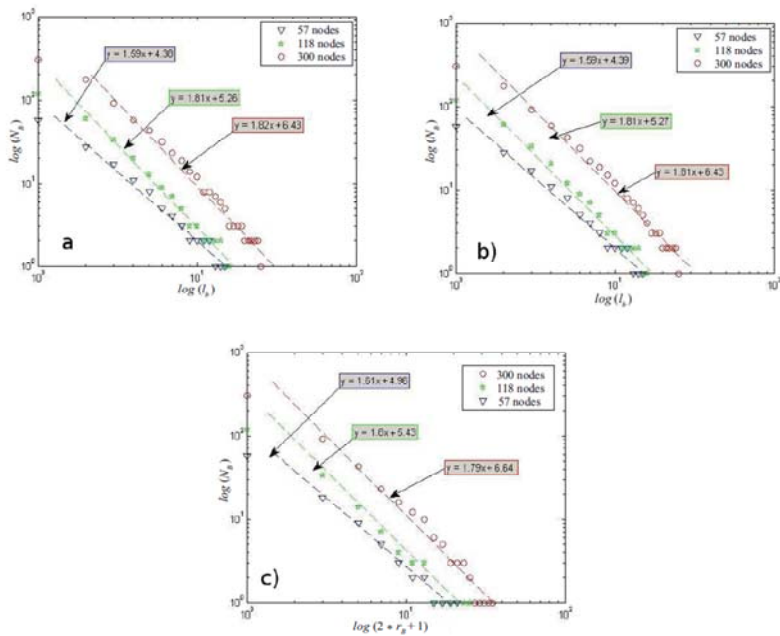


Figure 6.9. Results of the three algorithms applied to the IEEE 57-node, 118-node and 300-node networks: a) coloring algorithm (Greedy algorithm), b) CBB algorithm and c) MEMB algorithm

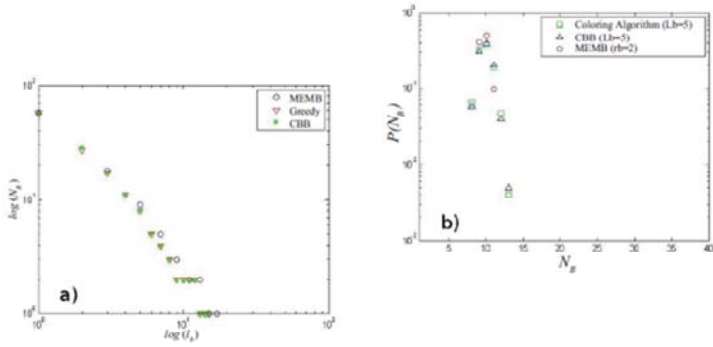


Figure 6.10. a) Comparison of the fractal dimensions obtained by the application of the three algorithms to the IEEE 57-node network (the number of executions of each algorithm is 10_2). b) Comparison of the distributions of the number of boxes N_B necessary to cover the IEEE 57-node network (the number of realizations of each algorithm is 10_3)

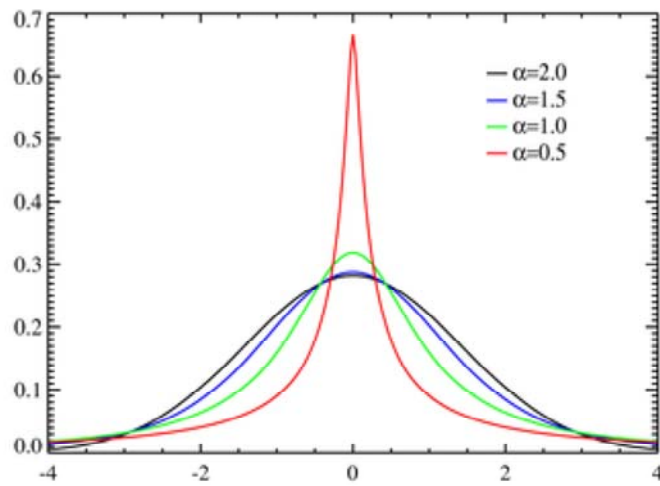


Figure 7.1. *Influence of the parameter α on α -stable probability distributions*

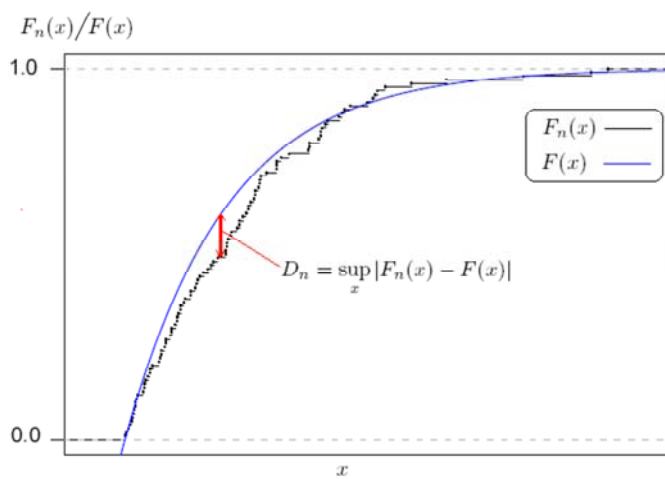


Figure 7.2. *The basic concept of the Kolmogorov–Smirnov test*

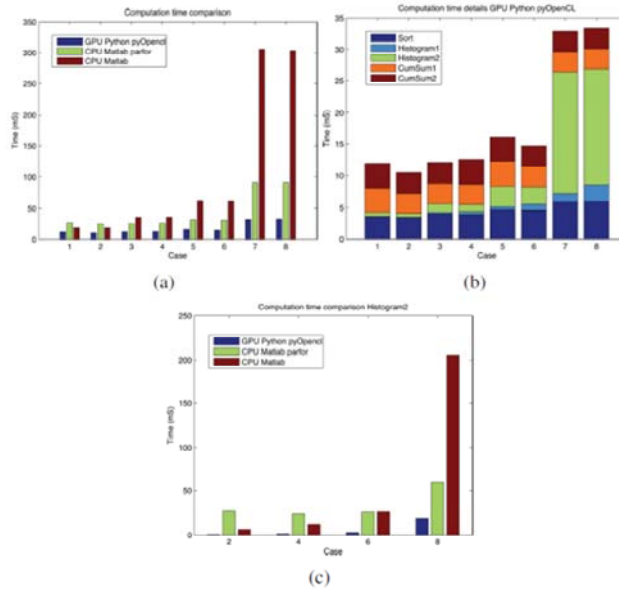


Figure 7.7. Execution time of the algorithm: a) comparison between GPU Python OpenCL, CPU Matlab in sequential and CPU Matlab in parallel, b) details of the GPU Python OpenCL algorithm and c) details of Histogram2. The tests are performed on different sizes of series X_1 and X_2 described in Table 7.21

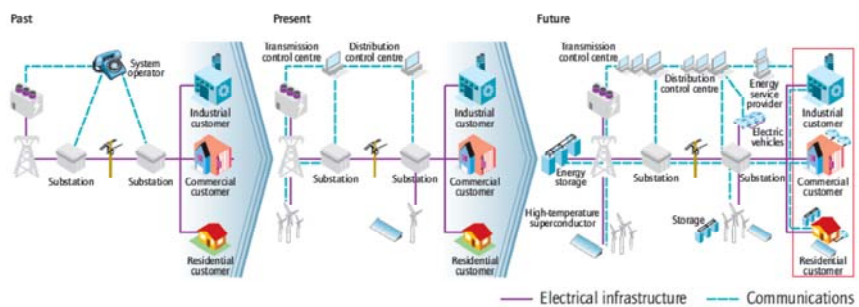


Figure 8.1. Smart electric systems [IEA 11]

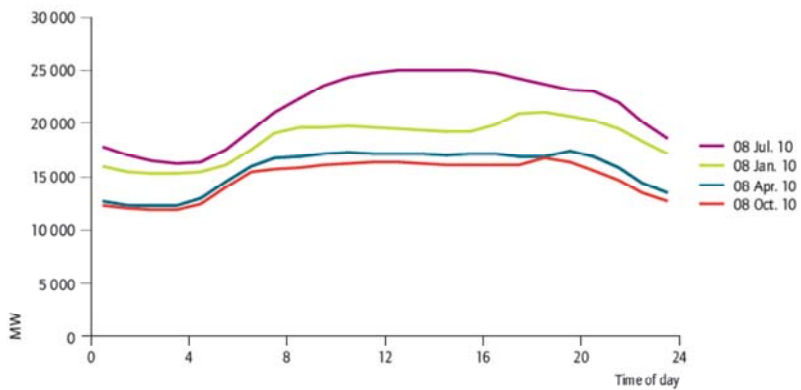


Figure 8.2. Example of a demand curve of the electricity system over 24 hours, corresponding to several dates of the year (source: data from the independent operator of the electricity network, Ontario, Canada [IEA 11])

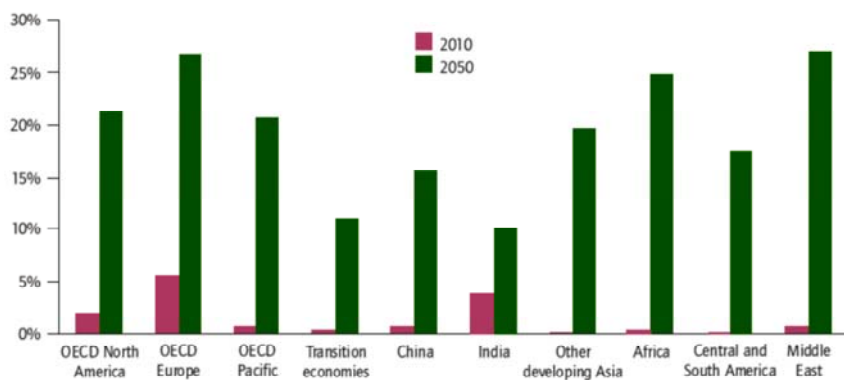


Figure 8.3. *Proportion of variable character energy production, by region (IEA Blue Map Scenario [IEA 11])*

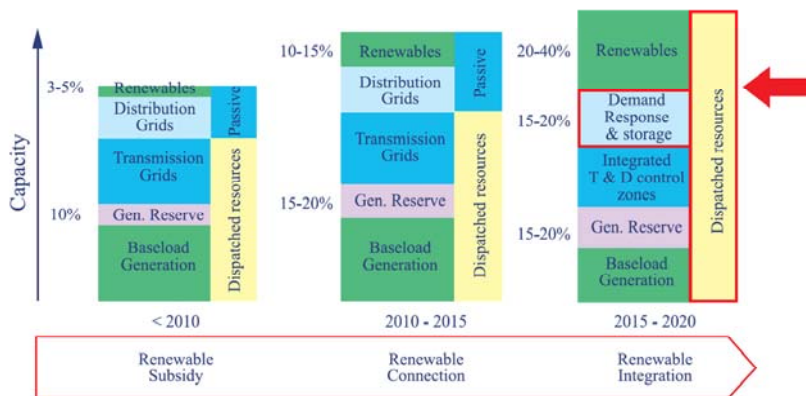


Figure 8.4. Development of Grid flexibility versus Variable Renewable Resources [FEN 09]

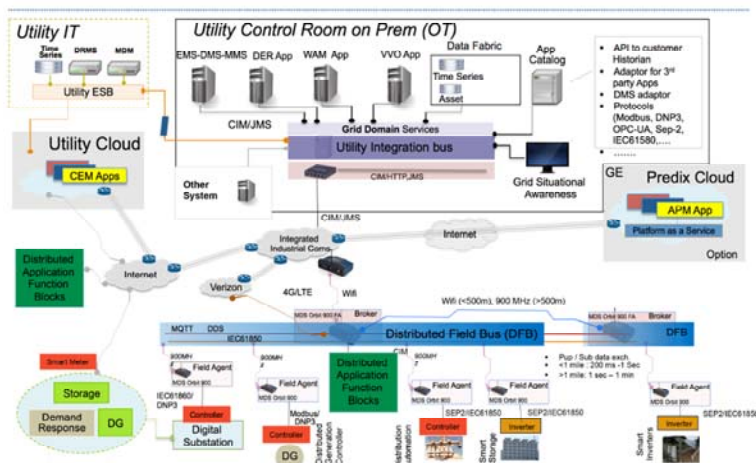


Figure 8.5. New generation of computerized platforms for Smart Grid deployment (source: GE Grid Solution 2016)

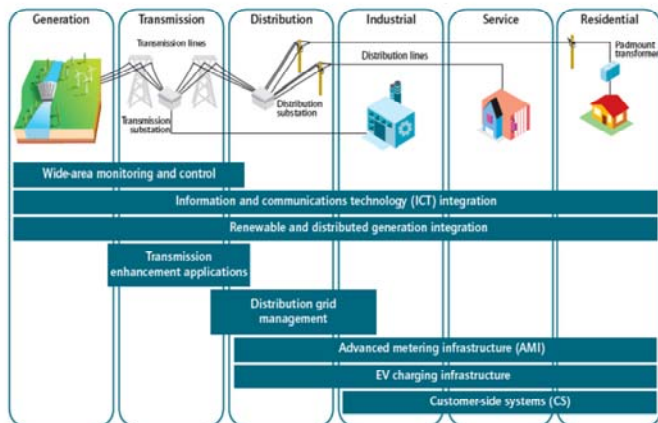


Figure 8.6. Smart Grid Technology areas (source: IEA Smart Grid Roadmap)

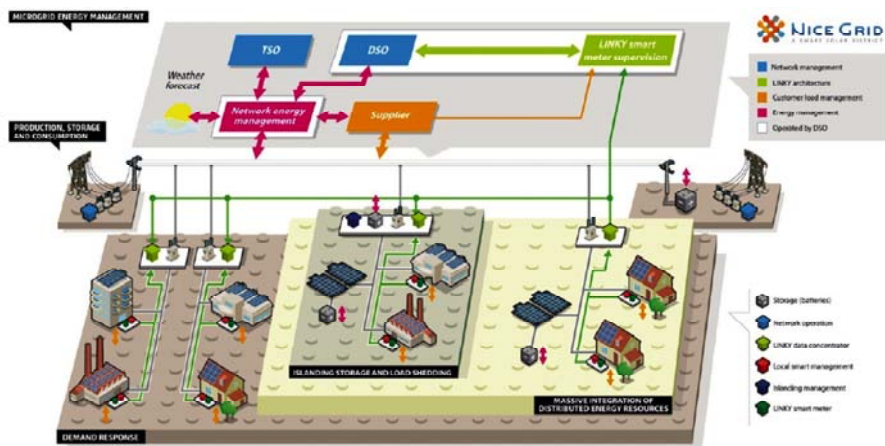


Figure 8.7. Smart Grid Technology areas [SOL 16]

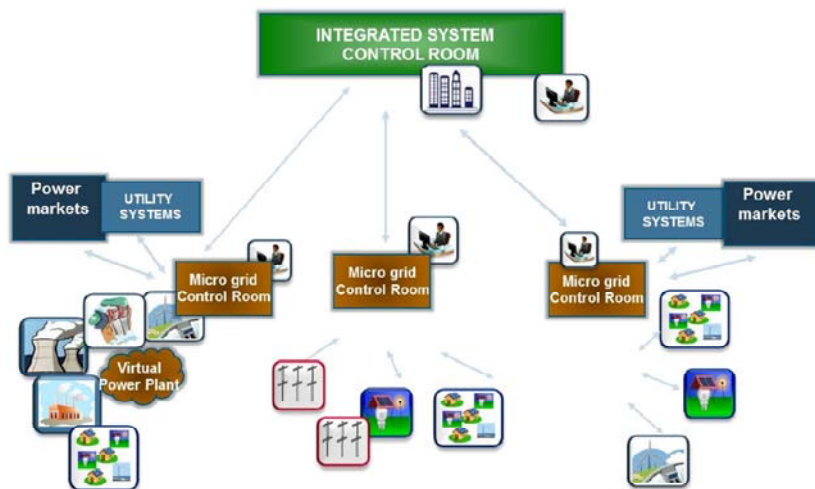


Figure 8.8. *Diagram of MicroGrid integration in the energy system*

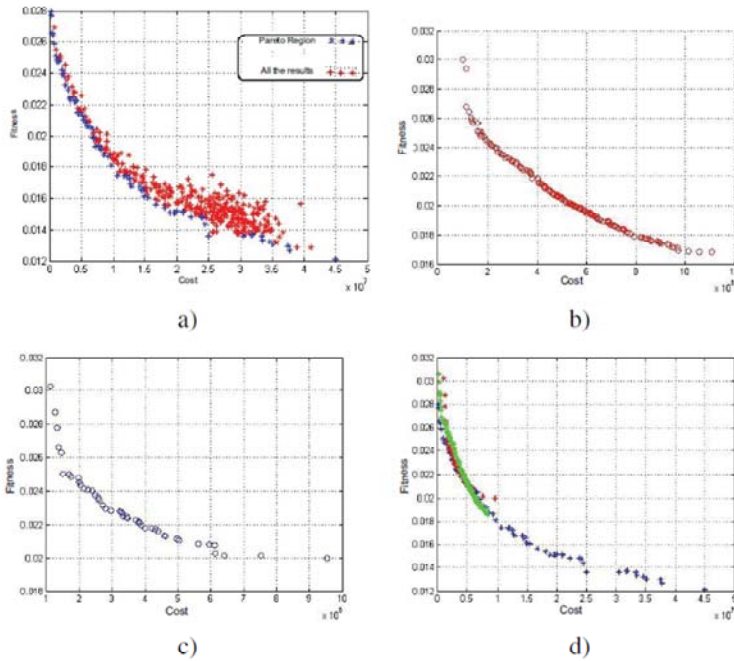


Figure A2.2. Illustration of the results obtained with the multi-objective case: a) Pareto front, _-Constraint approach, 35 particles and 500 iterations; b) Pareto front, H-GAPSO approach, 50 particles and 1,000 iterations; c) Pareto front, H-PSO approach 50 particles and 1,000 iterations. d) Pareto front, H-PSO approach (50 particles and 1,000 iterations), H-GA-PSO approach (50 particles and 1,000 iterations) and _-Constraint approach (35 particles and 500 iterations)